CFD investigation of a natural ventilation wind tower system with solid tube banks heat recovery for mild-cold climate

Miaomiao Liu [1], Carlos Jimenez-Bescos [1] and John Calautit[1,]*

[1]Department of Architecture and Built Environment, University of Nottingham, UK
*Correspondence: john.calautit1@nottingham.ac.uk

Abstract

Passive strategies are increasingly being employed in buildings to minimize their total energy consumption and emissions. Wind tower as a particular natural ventilation device can capture the wind flow from higher locations and supplies the air into the buildings' interior space without consuming electric power. But its use in mild-cold climate is very limited due to excessive heat loss and thermal discomfort. Limited research has previously been conducted to explore the pre-heating of the supply air in the wind tower to address the issue and potentially increase its adoption in mild-cold climate conditions. Therefore, a novel wind tower ventilation system integrated with solid tube banks heat recovery (HR) is proposed in this research. By combining with a passive heat recovery device, a wind tower can be operated in winter conditions to improve indoor ventilation while reducing the building heating energy consumption. A three-dimensional computational fluid dynamics (CFD) model is developed to investigate the effects of the longitudinal pitch (SL) and the transverse pitch (ST) of the HR device on the ventilation and thermal performance. The overall performance of the wind tower is evaluated under different outdoor wind speeds. The results show that the heat recovery can be improved by reducing SL and ST, raising the supply fresh air temperature by up to 6.4 °C. Furthermore, the proposed wind tower can provide sufficient ventilation for a typical classroom occupied by 15 people when the external wind speed exceeds 3 m/s.

Keywords: buildings; CFD; wind tower; heat recovery; passive strategy

1. Introduction

Buildings are responsible for about 40% of global energy consumption and will play an important role in reducing global energy use [1]. Space Heating, Ventilation and Air-conditioning (HVAC) accounting for almost two-thirds of the total energy use, have grown at an annual rate of 1.8% for 40 years [2]. The magnitude and potential growth of buildings energy demand are both significant. This represents a major opportunity to reduce energy consumption and greenhouse gas emissions [3][4]. Although reducing the use of mechanical HVAC can solve the issue, it is also important that the thermal comfort and indoor air quality are not compromised.

This challenge is more important now with the global pandemic, which raised awareness about the importance of indoor air quality. The UK government and World Health Organization (WHO) put a great emphasis on ventilating rooms to reduce the risk of virus transmission [5][6]. Hence, a balance between energy reduction and good comfort and air quality is necessary when developing energy-efficient strategies and technologies.

1.1 Literature review

Generally, there are three ways to ventilate, natural ventilation (i.e., window [7][8], wind tower[9][10], atrium [11][12], courtyard [13][14]), mechanical ventilation (i.e., fan [15] and air conditioner [16]) and hybrid ventilation [17][18]. Natural ventilation can offer considerable energy saving at energy saving s compared to mechanical ventilation as it mainly relies on buoyancy forces and wind effect. A good example of a natural ventilation device that is attracting the attention of researchers is the wind tower or windcatcher.

Wind tower provided passive cooling and ventilation in buildings in the Middle East for centuries. As early as 1984, Bahadori [19] investigated the natural ventilation and passive cooling performance of a new wind tower design. The feasibility of the proposed design was evaluated through theoretical calculation. The supply air velocity increased up to 5 m/s in the new design while the internal temperature was reduced to 15 °C. Moreover, the dust content in the air was reduced. Many of the studies focused on improving the cooling performance by incorporating evaporating cooling strategies. For example, Bouchahm et al. [20] explored the cooling performance of a single-sided wind tower integrated with evaporative cooling. The results demonstrated that the higher the height of the wet column and the smaller the size of conduits partition inside the wind tower, the higher the reduction in the air temperature, achieving a maximum temperature drop of up to 18.6 °C, highlighting the capability of the passive cooling strategy in a dry and hot climate.

While some of the studies focused on enhancing the ventilation performance by optimizing the wind tower design. Farouk [21] discussed the ventilation performance of square, hexagonal and six-opening circular cross-section wind towers. The external wind speed was the dominant factor in the induced air volume. The air velocity in the hexagonal windcatcher was 19% higher than that in the square, while the total air volume was nearly 20% less. It was also concluded that the square windcatcher was outstanding at providing thermal comfort. Recently, some research has combined the wind tower with other technologies, such as renewable energy system [22][23], solar chimney [24] and courtyard [25], to enhance its ventilation performance. Benhammou et al. [26] designed a wind tower assisted with an Earth-to-Air Heat Exchanger (EAHE) to improve its cooling effect. This system was tested in hot and arid regions of Algeria where the ambient temperature exceeded 45 ℃. It was concluded that increasing the pipe length positively affected on the cooling efficiency, but the pressure loss also increased. Ghoulem et al. [27] looked into the cooling potential of the wind tower with a passive downdraft evaporative cooling system in the greenhouse in hot climate. Different wind speeds in the range of 1.96 and 6.07 m/s and different ambient temperatures ranging from 30 ℃ to 45 ℃ were considered. The results indicated that the proposed wind tower system could reduce the average indoor temperature by 17.13 ℃. As observed from the literature, many studies explore wind towers in hot regions designed to provide passive cooling and ventilation.

While different research groups [28-30] employed heat transfer devices to enhance the thermal performance of the wind tower. Calautit et al. [28] designed a wind tower system incorporating heat pipes to improve thermal comfort in hot and dry climates. This system could potentially reduce the supply air temperature by 13-15 ℃. The simulation results denoted that the internal airflow rate was lowered by 7% and 10% with the heat pipes arranged in different orientations. Besides, the airflow velocity was impeded after adding heat pipe heat exchanger. Hughes et al. [29] also studied the pre-heating and pre-cooling ability of the heat pipe heat exchanger in a natural ventilation system. The research identified that under the optimal pattern, the fresh air temperature could be lowered by 15.6 ℃ or improved by 3.3 ℃, highlighting its potential in reducing the carbon footprint of domestic buildings. Furthermore, Calautit al. [30] examined the ability of the rotary thermal wheel to recover heat from exhaust air and pre-heating fresh incoming airflow, to improve the use of wind towers in mild-cold climates. Experimental and CFD results demonstrated that the wind tower ventilation system could provide the recommended fresh air rate in a low outdoor wind speed (1.5 m/s). The heat recovery system could raise the indoor air temperature by up to 3.7 ℃, but it was also pointed out that incorporating the heat recovery wheel caused a reduction in the indoor air velocity by 14% to 30%. Table 1 summarizes the wind tower development in providing passive cooling and heating effect.

Table 1. Summary of the wind tower development in passive cooling and heating

Ref	Climate	Focus	Methodology	Results
Bahadori [19]	Hot and arid	Passive cooling effect	Theoretical analysis	Using clays inside the wind tower could reduce the internal temperature by 15 ℃. Moreover, the indoor dust content was reduced.
Bouchahm et al. [20]	Hot and dry	Ventilation and passive Cooling	Theoretical analysis and field experiment	With a higher height of the wetted column and smaller size of the conduits partition could achieve the maximum temperature drop of 18.6 ℃ and the relative humidity by 62.6%.
Farouk [21]	Not applicable	Ventilation	CFD simulation	The air velocity in the hexagonal windcatcher was 19% higher than that in the square, while the total air volume was nearly 20% less. It was

				concluded that the square windcatcher was outstanding at providing thermal comfort.
Chel et al. [22]	-	Passive heating and cooling	-	Combining with the solar passive building techniques can tremendously reduce the heating/cooling energy consumption as well as the CO_2 emission.
Sakhri et al. [23]	Cold to hot and arid	Passive heating and cooling	Field experiment	Assisted with the EAHE and solar chimney, the wind tower was able to reduce the indoor air temperature by 13 °C in summer and raise it by 10 °C in winter in Algeria. Besides, the relative humidity ranged from 14%-76% in winter but it did not exceed 27% in summer conditions.
Moosavi et al. [24]	Warm and arid	Ventilation and passive cooling	CFD simulation and lab experiment	Integrated with the solar chimney and water spray, the wind tower decreased indoor temperature by 5.2 °C, saved 75% the cooling energy and reduced 90% of the ventilation energy in the prototype building.
Benkari et al. [25]	Hot	Ventilation	CFD simulation	After integrating the wind tower with a semi-enclosed courtyard, the ventilation rate could be 100% higher than the required rate.
Benhammou et al. [26]	Hot and arid	Passive cooling	Theoretical calculation	Coupling EAHE to the wind tower enhanced the cooling effect but also led to increasing pressure loss.
Ghoulem et al. [27]	Hot	Passive cooling	CFD simulation	The wind tower with a passive downdraft evaporative cooling system could reduce the average indoor temperature by 17.13 °C.
Calautit et	Cold	Passive	CFD simula-	Introducing the heat pipes

al. [28]		heating	tion and lab experiment	heat exchanger into the wind tower raised the supply temperature by 4.5 K. It should also be noticed that the air supply rates was 8%–17% lower.
Hughes et al. [29]	Hot and arid	Passive heating and cooling	CFD simulation	The supply fresh air temperature was lowered by 15.6 ℃ or improved by 3.3 ℃ by the wind tower equipped with heat pipes.
Calautit et al. [30]	Mild-cold	Passive heating	CFD simulation and lab experiment	The wind tower that incorporated passive heat recovery wheel could improve the indoor air temperature by up to 3.7 ℃, but a reduction in the indoor air velocity of 14% to 30% was also observed.

1.2 Novelty and gap in knowledge

Of the literature reviewed here, a superior advantage of a wind tower is that it can provide ventilation and cooling without consuming electric power. However, the limitations of the wind tower system cannot be ignored. In winter, for example, especially in mild and cold climates, the operation of wind towers may lead to ventilation heat loss and thermal discomfort. This would lead to the system not being operated during the heating season. There is currently limited research investigating the integration of passive heat recovery and air pre-heating.

Although some research introduced heat transfer devices such as rotary thermal wheel and heat pipes into wind tower design, no work has explored more simple types of heat exchange technologies that could be lower cost and does not require moving parts to operate like the rotary wheel and working fluids such as heat pipes. Also, few studies explored the application of wind tower systems in mild-cold climates. Therefore, this study proposed a novel design of windcatcher incorporating solid tube banks HR, highlighting its application potential in mild-cold climates. Tube heat exchanger does not rely on working fluid to transfer heat, and has high heat transfer performance, is easy to operate, does not have moving or rotating parts and is in low cost.

1.3 Aims and objectives

To fill the research gap as discussed, a novel wind tower system integrated with solid tube banks HR was proposed in this study. The aim was to improve the wind tower's ability to function throughout the year, especially in temperate climates with mild to cold winters. A CFD model was developed and validated to evaluate the proposed wind tower system's heat recovery and ventilation performance. The impact of parameters such as the longitudinal pitch (SL) and transverse pitch (ST) was evaluated. Furthermore, the potential reduction in heating load for a typical room occupied by 15 people due to the addition of the solid tube banks HR was also estimated.

2. Problem description

The proposed wind tower system schematic with solid tube banks HR device was depicted in Fig. 1a. We considered a three-dimensional uniform flow around and into the four-sided wind tower with HR. A four-sided wind tower was the most common type capable of catching the wind and supplying fresh air irrespective of the wind in all directions [31]. The wind tower was designed with a height of 2.2 m, width of 1 m and length of 1 m. Louvers were located at the openings of the wind tower allowing the air to pass through which was angled at 45° with a regular interval of 0.1 m. The wind tower was considered fully open so that the dampers at the bottom were not modeled. As shown in Fig. 1b, the HR device consisted of 8-layer solid copper tubes with a staggered arrangement. The diameter and length of each tube were set as 0.02 m and 1 m, respectively. SL and ST represented the longitudinal pitch and transverse pitch equal to 25 mm and 60 mm, respectively. The schematic of the dimensions of the solid tube HR device was presented in Fig. 1c.

The proposed wind tower was mounted on the roof of a small classroom occupied by 15 people with a height ×width ×length of 3 m ×5 m ×5 m, constituting a micro-climate. For all simulations, we fixed the outdoor air temperature at 5 °C, assuming a typical temperature during the winter in the UK [32]. The incoming wind direction was perpendicular to the opening of the wind tower. The external fresh air entered the wind tower through the openings with louvers and was redirected down into the room. After mixing with the indoor air, the exhausted air was discharged from the other openings of the wind tower. The introduction of HR device can reduce the ventilation heat loss and recover some of the heat exhausted by the wind tower used to pre-heat the supply of fresh air. The wind tower system was located in the middle of the wind tunnel section (5 m× 5 m ×10 m) with the upstream distance equal to the downstream distance, similar to the experimental set-up in Calautit et al. [33]. The dimensions of the geometry are summarized in Table 2.

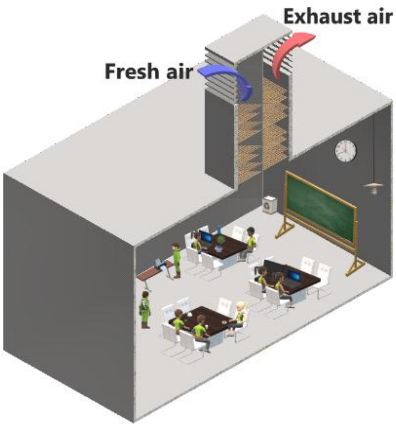

(a)

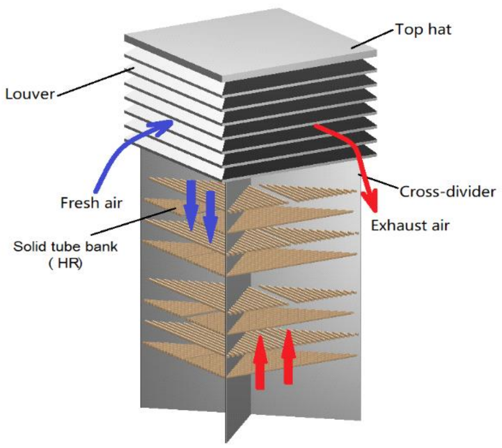

(b)

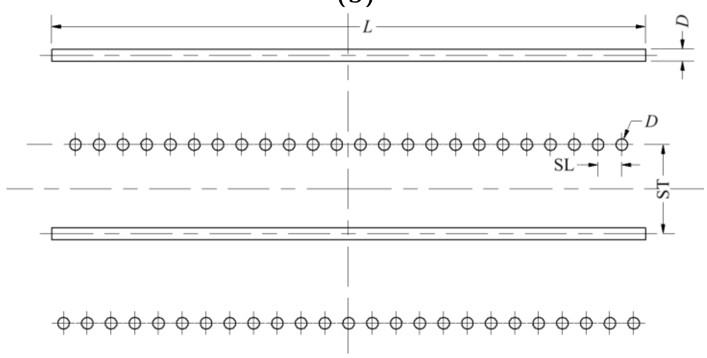

(c)

Fig. 1 (a) The schematic of the three-dimensional model of the proposed wind tower system; (b) the detailed view of the solid tube banks; (c) the dimension diagram of the HR device

Table 2. Summary of the geometrical dimension

Parameter	Value
Height, width and length of the room (fluid domain)	3, 5, 5 m
Height, width and length of the wind tower with HR (fluid domain)	2.2, 1, 1 m
Height, width and length of the wind tunnel (fluid domain)	5, 5, 10 m
Louver angle	45˚
Louver height	0.7 m
Louver layers	7
Longitudinal pitch (SL)	25-45 mm
Transverse pitch (ST)	60-180 mm
Tube diameter (*D*)	20 mm
Tube length (*L*)	1 m

3 Methodology

3.1 Boundary conditions

The commercial software ANSYS Fluent (version 18.1) was used to conduct the CFD simulation. Because real climate conditions changed over time which can be complex to model, several assumptions were made to simplify the simulation [34].

(1) Flow regimes inside and around the wind tower and the room were considered fully turbulent. The wind direction angle was assumed to be constant at each fixed wind speed.

(2) The fluid domain was considered steady and incompressible. The physical properties of the airflow remained unchanged.

(3) Radiation and infiltration were neglected in this study with mainly considering the ventilation heat loss.

The governing equations have been discussed in many literatures and are not repeated in this study[28][29][30]. The outdoor air at a constant temperature of 5 °C entered into the integrated system from the inlet of the wind tunnel domain with a uniform velocity profile [28]. A pressure outlet was implemented in the outlet. The heat flux of the room floor was set to 30 W/m^2 to simulate the effect of the heat gains from occupants, lighting and equipment in a typical classroom [30]. SIMPLE algorithm was used for pressure-velocity coupling [33]. No-slip boundary condition was applied to all walls [33]. The momentum equation adopted the second-order central difference scheme, and the turbulent kinetic energy and turbulent energy dissipation rate equations used the second-order upwind scheme. Many researchers have demonstrated that RNG k-epsilon turbulence model was superior to other turbulence models in simulating flow over tube heat exchangers. For instance, Nakhchi and Esfahani [35] indicated that the numerical results obtained with RNG k-epsilon were more accurate for simulating the heat transfer performance of tube heat exchangers. A number of research work also showed that the RNG model had higher accuracy in terms of heat transfer prediction [36][37]. In terms of natural ventilation, large eddy simulation (LES) was intrinsically more accurate in predicting airflow velocity and volume flow rate mentioned by Blocken [38]. However, LES also required more computational power as well as higher computational time. Many studies have highlighted that the RNG k-epsilon model improved the calculation efficiency while ensuring simulation accuracy and reliability. It was a model suitable for many flow problems in engineering [39][40][41]. As for the wind tower simulation, RNG also represented sufficient accuracy when compared with the experimental results [42][43][44]. Therefore, the RNG model was more suitable for this research. Standard wall function was implemented in the near-wall treatment [45]. Roughness height and roughness constant were 0.001 mm and 0.5. The boundary conditions of the computational domain are shown in Fig. 2. The CFD parameters are summarised in Table 3.

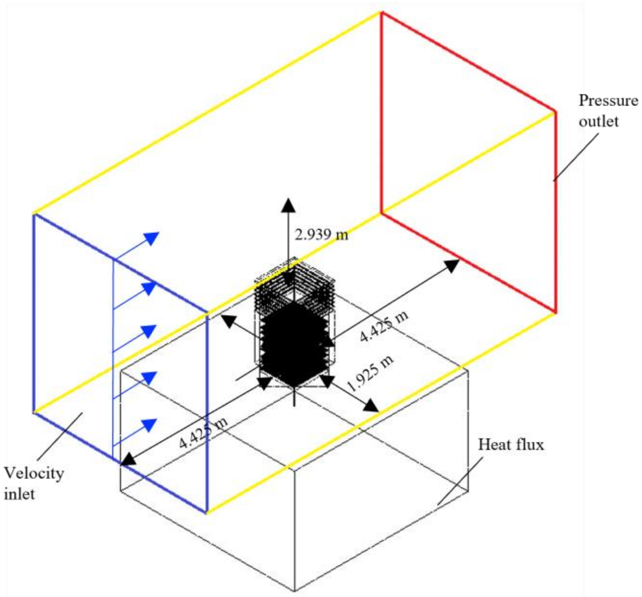

Fig. 2. Boundary conditions of the computational domain

Table 3. Summary of the CFD parameters [33]

Time	Steady-state
Gravity (m/s^2)	-9.81
Turbulence model	RNG k-epsilon
Wall function	Standard
Velocity inlet (m/s)	1-5 (uniform)
Temperature inlet (K)	278
Pressure outlet	Atmospheric
Heat source (W/m^2)	30
Wind direction angle (°)	0
Wall	All walls: no slip
Roughness height	Macro-micro climate walls: 0.001 mm
Roughness constant	All walls: 0.5

3.2 Mesh generation and mesh independence analysis

The geometry model in Fig. 1 was imported into ANSYS DesignModeler to generate the fluid domain. A tetrahedral mesh was adopted and the mesh refinement, with 0.01m element size, was implemented to the surfaces of the wind tower system. Curvature refinement was applied to all surfaces and edges to better capture the air-flow characteristics around sharp areas. The mesh growth rate is set to 1.20. The obtained mesh quality was 0.84 with the maximum skewness kept lower than 0.85 and the number of elements was 18,642,314. Fig. 4 presented the surface mesh of the louvers and solid tubes.

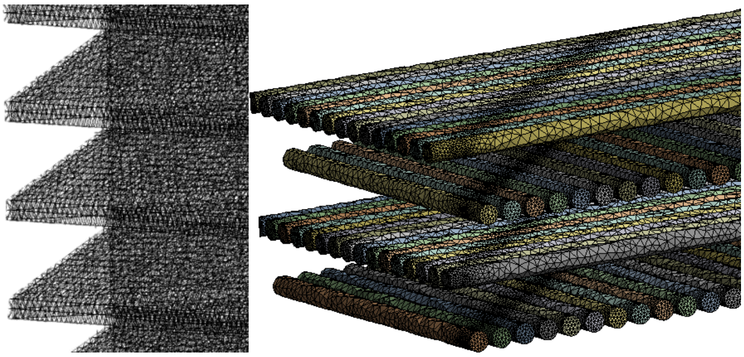

Fig. 4 Surface mesh of the louvers and solid tubes

In order to reduce the influence of mesh on simulation accuracy, mesh independence analysis should be carried out until the difference between the simulation results becomes insignificant. Six different mesh numbers, from coarse to fine, were tested with the simulation results shown in Fig. 5. The main concerns in the presented work were the velocity, pressure and temperature fields. When the number of elements increased from 14 million to 21 million, the values of air velocity and air temperature almost remained unchanged with the maximum variation of 7%. Hence a total mesh elements number of 17 million was considered for this study. Besides, a y+ value of 65 was obtained over walls. The log law should basically be applied to the region corresponding to 30<y+<300. Although the y+ value in the present work was not the most desirable, it still satisfied the requirements [46].

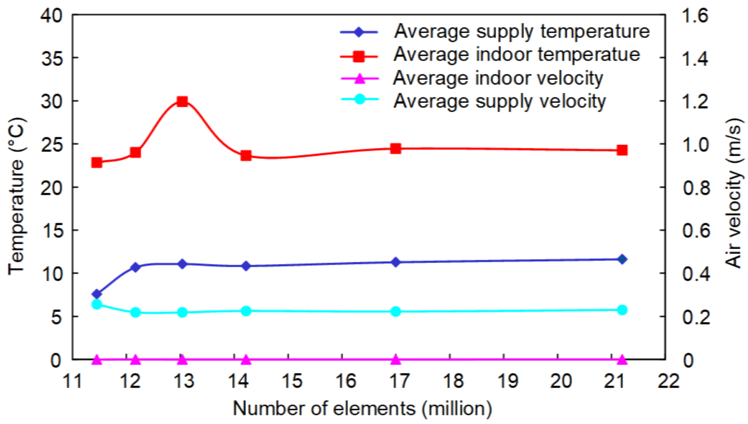

Fig. 5. Mesh independence analysis

3.3 Validation of the wind tower CFD model

In order to carry out modelling work, the CFD model should be verified and validated to ensure the reliability of the simulation results. The four-sided wind tower used in Calautit et al. Ref. [33] was mounted to the roof of a test room. The experimental model was then integrated into a wind tunnel to simulate the external wind. The geometry of the standard wind tower in the wind tunnel was shown in Fig. 6.

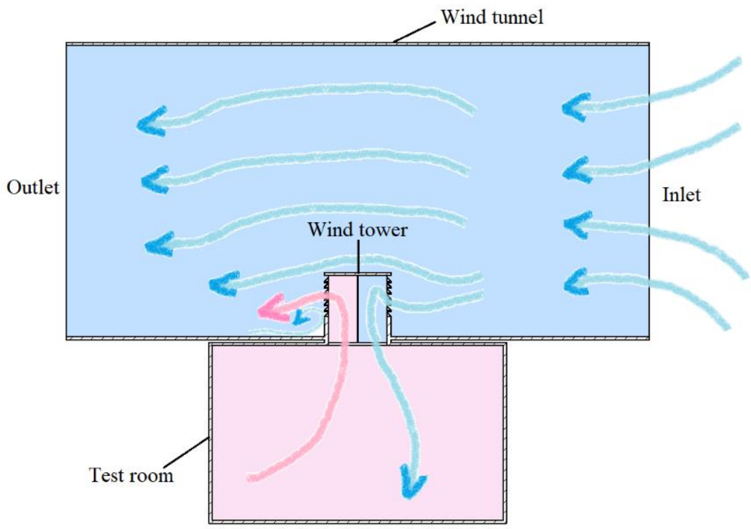

Fig. 6. The geometry configuration of the standard wind tower [33]

Fig. 7a showed the average indoor air velocity values and contours represented by 9 sample points in the CFD simulation and the experiment conducted by Calautit et al [33]. A similar overall trend can be observed. The maximum air velocity in the middle of the room was obtained with a value of 1.08 m/s in the simulation and 1.0 m/s in the experiment. Among these sample points, the air velocity at points 4, 5 and 6 in the CFD simulation was almost consistent with the experimental values. However, CFD underestimated the values of indoor velocity slightly at the remaining six points, which accounts for the large overall average error. Fig. 7b also presented the velocity vectors on the plane of y=1.55 m. As can be seen, flow separation mainly occurred around points 1, 2, 3, 7, 8 and 9, resulting in low-speed vortex regions.

Fig. 8a displayed the simulated streamline contour in the wind tower and tested room. Fig. 8b presented the flow pattern recognized in the smoke visualisation tests

[33]. The flow characteristics in the CFD model and experiment was basically consistent. As observed, the air flowed smoothly around and above the tower. Some of the air entered the wind tower supply channel through 45 ° louvers and subsequently, the was directed towards the floor of the below room. When the air hit the bottom surface, the air velocity slowed down and diffused to the side walls, forming several low-speed vortex regions. The deviation between the numerical and experimental was because Reynolds-averaged Navier-Stokes (RANS) model had some limitations for complex flow, such as jet, separation, thermal plume, etc. as mentioned before.

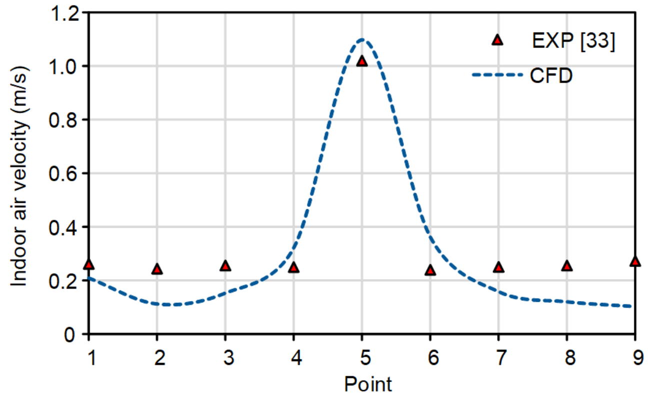

(a)

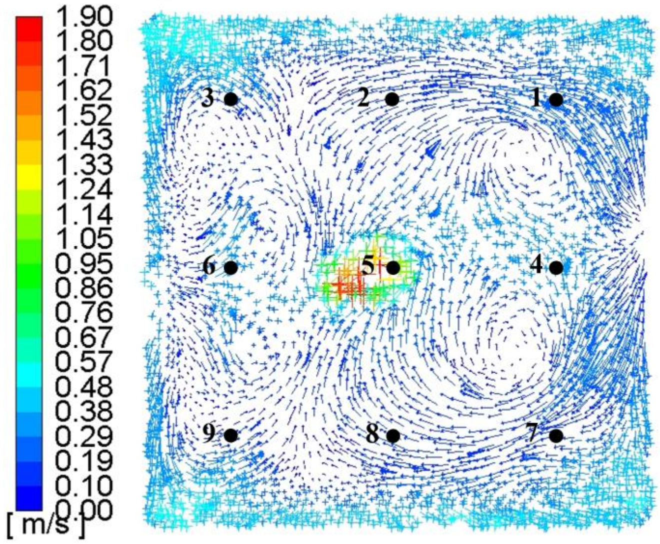

(b)

Fig. 7 (a) Indoor air velocity (points 1-9) when the outdoor wind speed was 3 m/s: CFD and experiment (Ref. [33]); (b) indoor velocity vector (y=1.55 m)

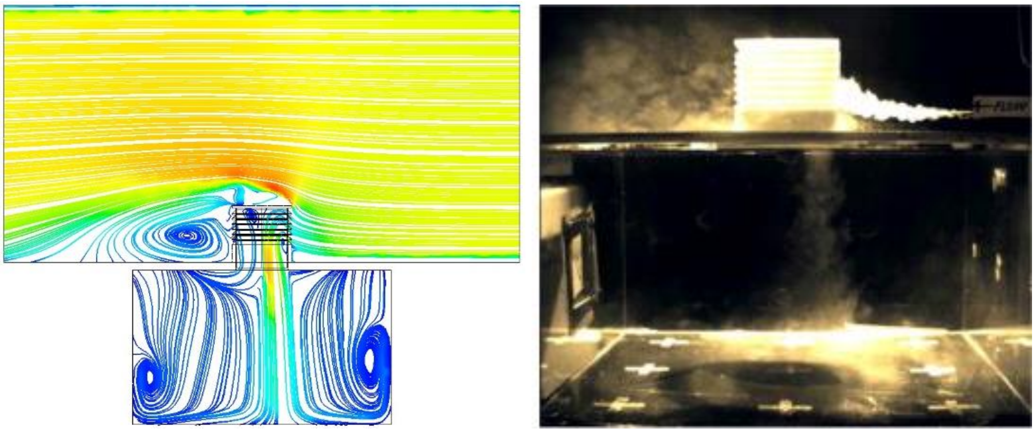

(a) (b)

Fig. 8 (a) The CFD streamline contour of a cross-sectional plane when the outdoor wind speed was 3 m/s; (b) flow pattern in the smoke visualisation tests (Ref. [33])

Fig. 9a compared the CFD predicted supply and exhaust air velocity values with the experimental data measured by Calautit et al [33]. Fig. 9b showed the velocity vectors in the supply and exhaust channels at the plane of y=3.05 m. Points 1, 2, 3 and 4 were located in the supply quadrant and the other three quadrants were exhaust outlets. The average supply velocity was 1.58 m/s, which was higher than the average exhaust air velocity of 0.58 m/s, which is the case for the four-sided wind tower at 0° angle. The patterns observed here were consistent with the observations in the experimental study of [33]. Overall, the supply and exhaust air velocity in CFD simulation fluctuated around the experimental results, with an average error of 25% which was acceptable for this type of study [47].

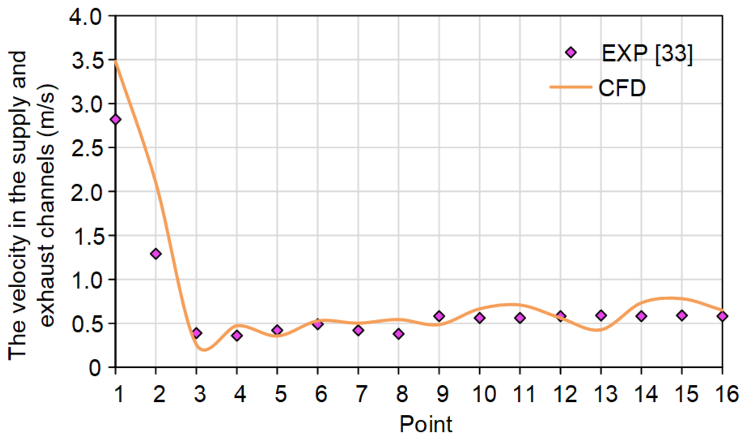

(a)

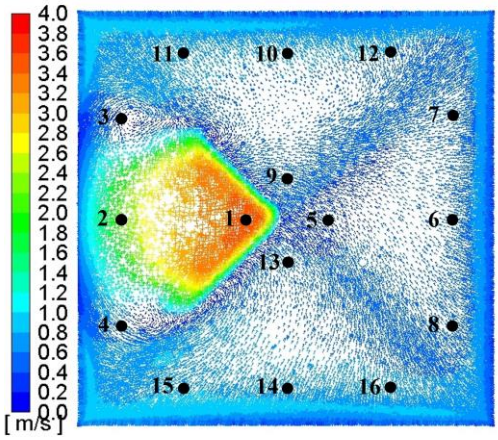

(b)

Fig. 9 (a) The velocity in the supply and exhaust channels when the outdoor wind speed was 3 m/s: CFD and experiment (Ref. [33]); (b) velocity vector at the supply and exhaust channels (y=3.05 m)

Fig. 10a compared the temperature difference between indoor and outdoor in CFD simulation and experimental measurement [28]. The indoor temperature is depicted by 9 sample points on the plane of y=1.55 m, as shown in Fig. 10b. The trend observed in the CFD simulation and experiment is basically consistent. But CFD values are slightly lower than the experimental results over the 9 sample points, with the error ranging from 1.2 °C to 3.2 °C. The lowest air temperature difference is observed in point 5, about 4 °C in CFD and 5.2 °C in experiment, in which the airflow velocity and ventilation heat loss are higher.

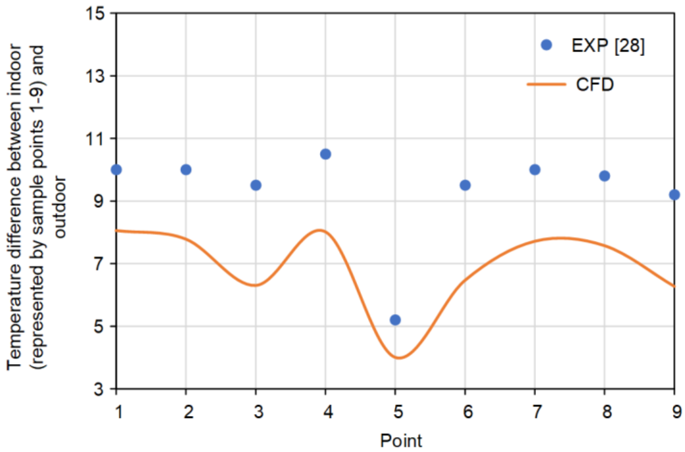

(a)

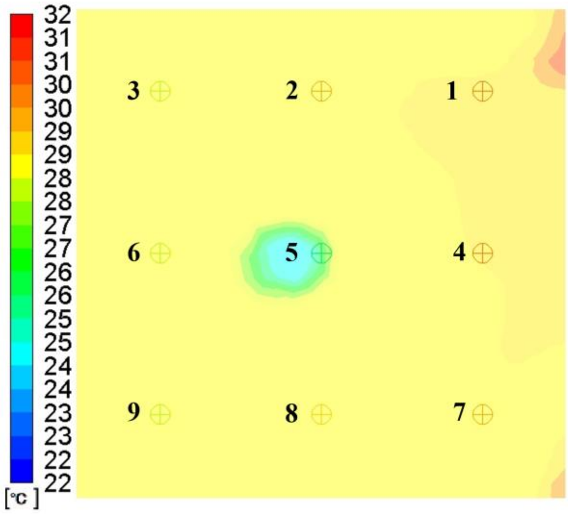

(b)

Fig. 10 (a) Indoor air temperature (points 1-9) when the outdoor wind speed was 2 m/s: CFD and experiment (Ref. [28]); (b) indoor temperature contour (y=1.55 m)

4. Results and Discussion

4.1 Overall airflow distribution

This section compares the airflow velocity, pressure and temperature distribution between the standard wind tower and the wind tower with HR. Several sample points are created to measure the supply and indoor air velocity and temperature. Table 4 gives the positions of supply and indoor sample points.

Table 4. Air velocity and temperature at supply sample points

Supply sample points	Coordinate x, y, z (m)
1	(-0.25, 3.085, -0.375)
2	(0, 3.085, -0.375)
3	(0.25, 3.085, -0.375)
4	(-0.125, 3.085, -0.25)
5	(0, 3.085, -0.25)
6	(0.125, 3.085, -0.25)
7	(0, 3.085, -0.125)

The velocity vectors of the cross-sectional plane (x=0) at the middle of the test room and at the supply channel are compared for the standard wind tower (Fig. 10) and the wind tower with HR (Fig. 11) at an inlet velocity of 1 m/s. As shown in Fig. 10a, part of the inlet air flows over the top of the wind tower, and a low-speed vortex zone is generated in the windward of the wind tower. Some of the air flows into the tower through the openings with louvers. The air flow accelerates along the shaft up to 1.2 m/s and as soon as it enters the test room below, the airflow velocity begins to decrease so that the average indoor air velocity is 0.12 m/s. By observing the velocity distribution inside the room, it can be seen that wind speed in the middle area is the highest while the velocity near the walls is much lower, in which flow separation occurs. As shown in Fig. 10b, one quadrant supplies fresh air and other three quadrants discharge exhausted air. The average supply air velocity is 0.78 m/s which is higher than the exhaust air velocity a little bit. This has always been a limitation of wind tower in a low outdoor wind speed. A similar overall velocity distribution can be observed in the wind tower with HR (Fig. 11), but it is clear that the supply and indoor air velocity are reduced with the values of 0.22 m/s and 0.02 m/s, respectively. This is because the addition of HR device leads to an increase of airflow resistance.

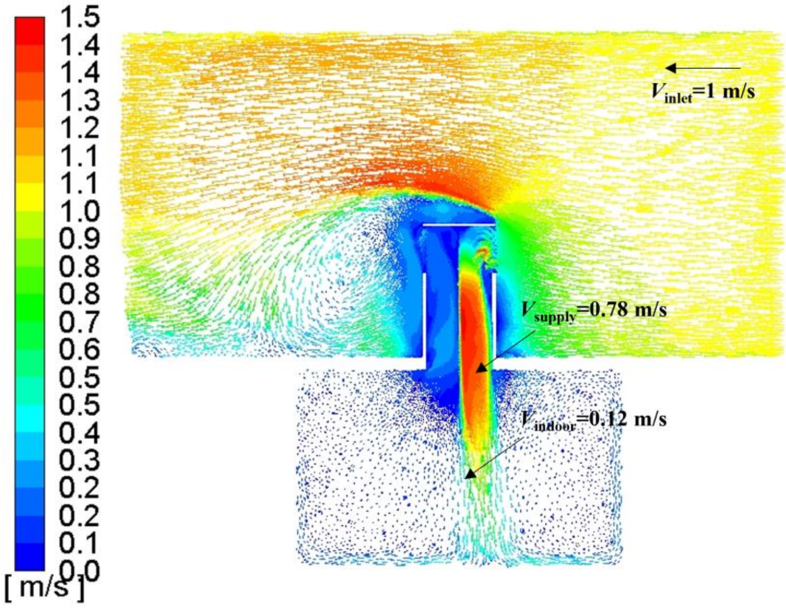

(a)

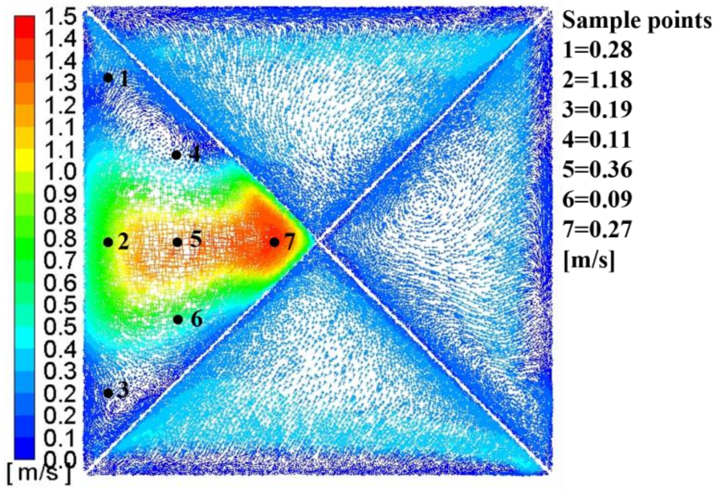

(b)

Fig. 10. Velocity vectors in the standard wind tower at the inlet velocity of 1 m/s: (a) the cross-sectional plane (x=0) and (b) the supply channel

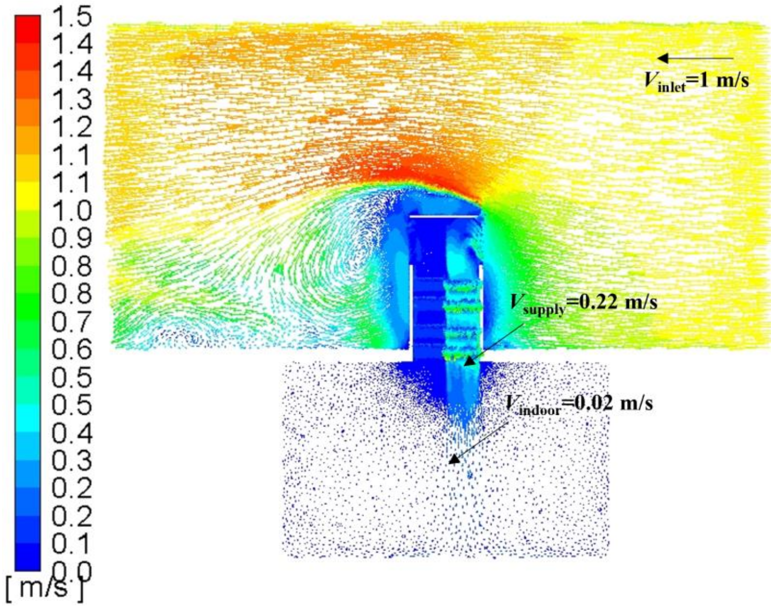

(a)

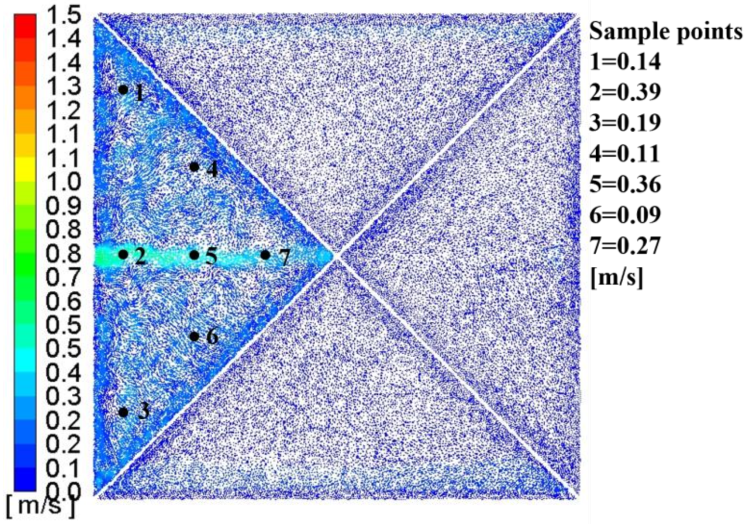

(b)

Fig. 11. Velocity vectors in the wind tower with HR at the inlet velocity of 1 m/s: (a) the cross-sectional plane (x=0) and (b) the supply channel

Figs. 12 and 13 compare the cross-sectional air temperature contours at the middle of the test room of the standard wind tower and the wind tower with HR at an inlet velocity of 1 m/s. From Fig. 12, it can be seen that due to the effect of the indoor heat gains and natural ventilation, the average indoor temperature reaches up to 9.2 °C, which would clearly cause discomfort. Moreover, it is should be noted that the simulation is not taking into account the heat loss from wall, roof, etc., but mainly considering ventilation heat loss. However, after integrating the heat recovery device into the wind tower, the indoor temperature can increased to 24.5 °C, as shown in Fig. 13, raising the temperature by up to 15.3 °C. The indoor temperature increase is mainly due to the heat gains from the internal heat sources and the reduction of ventilation heat loss. The heat recovery devices installed in the wind tower are expected to minimize and reuse some of the energy exhausted by the wind tower. Besides, according to the observed flow pattern in Fig. 12, the jet stream in the middle has the lowest air temperature in the space, which obviously leads to thermal discomfort in this location. For the wind tower with HR, temperature distribution has changed. Because of the existence of the HR devices, the airflow slows down, and the contact time with the HR devices increases

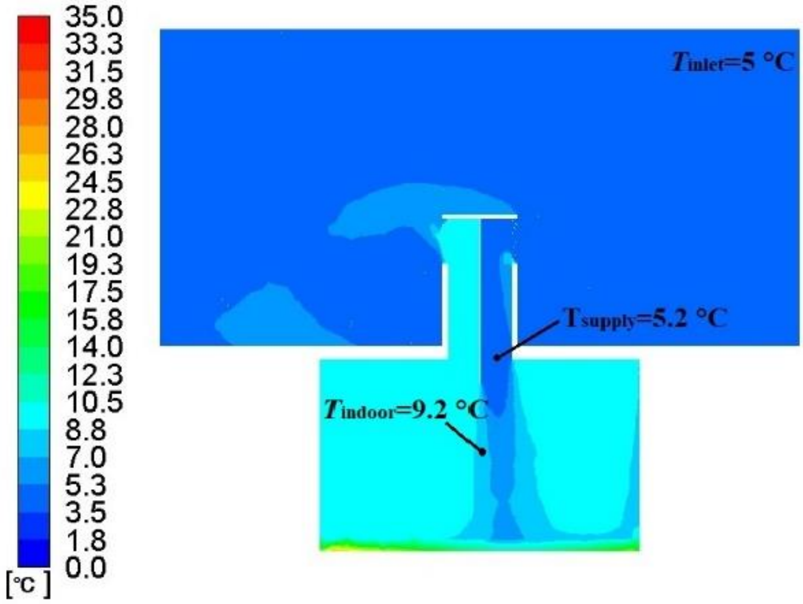

(a)

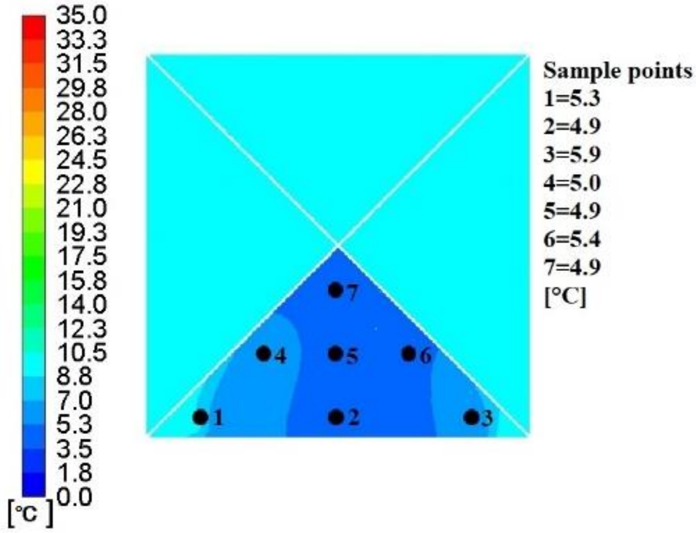

(b)

Fig. 12. Temperature contour in the standard wind tower at the inlet velocity of 1 m/s: (a) the cross sectional plane (x=0) and (b) the supply channel

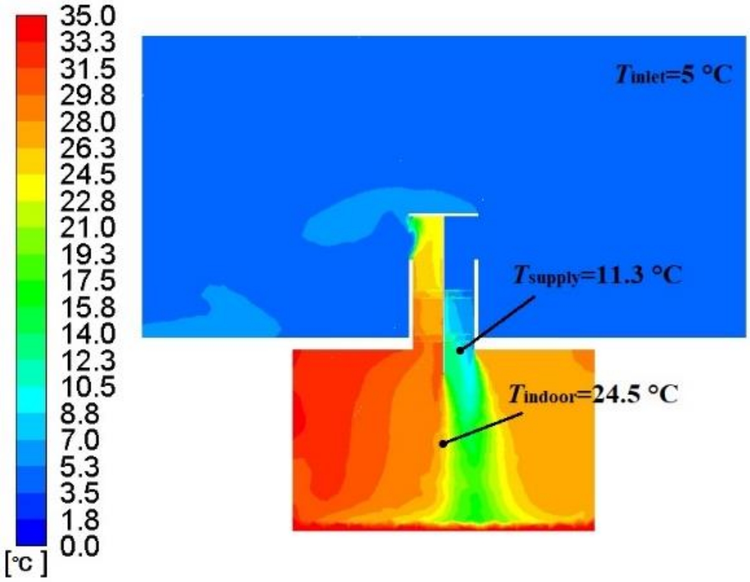

(a)

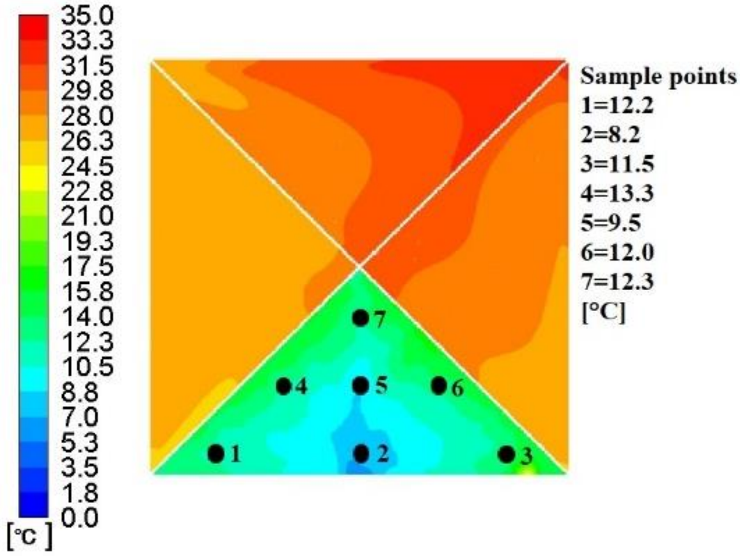

(b)

Fig. 13. Temperature contour in the wind tower with HR at the inlet velocity of 1 m/s: (a) the cross-sectional plane (x=0) and (b) the supply channel

Fig. 14 shows the pressure contour of a cross-sectional plane parallel with the inlet wind direction. It is observed the room is under negative pressure, with about 0.36 Pa in Fig. 14a and 0.38 Pa in Fig. 14b, which means that the supply rate was lower than the exhaust rate. The multi-directional wind tower has 4 quadrants, and at Under the wind direction angle of 0°, one of the quadrants acts as a supply channel, and the other three quadrants exhaust the indoor air. Furthermore, heat recovery devices reduce the airflow, and the impact on the pressure distribution can be observed in Fig. 14b.

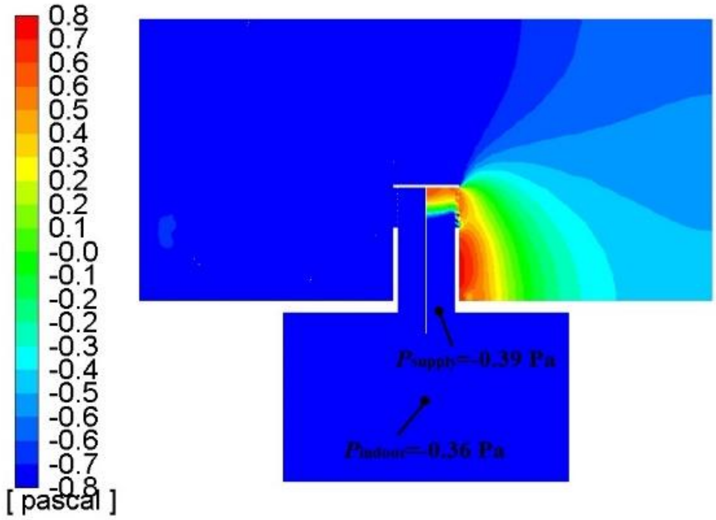

(a)

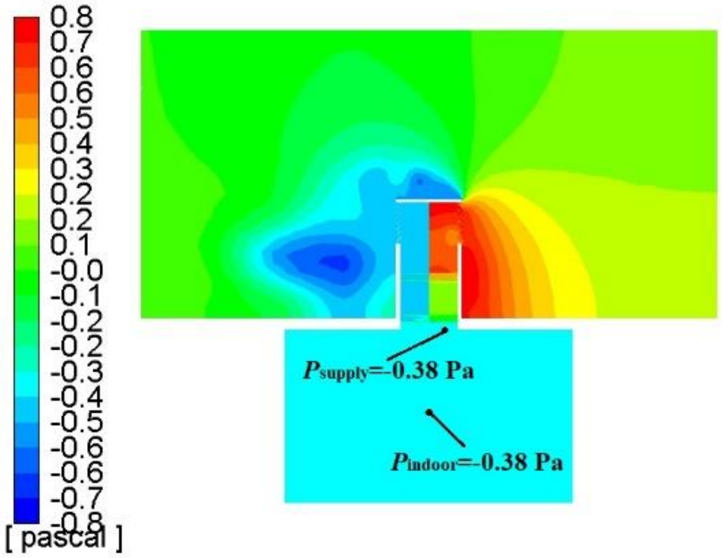

(b)

Fig. 14. Pressure contour of a cross-sectional plane with an inlet velocity of 1 m/s: (a) the standard wind tower and (b) the wind tower with HR

4.3 Effect of longitudinal pitch SL and transverse pitch ST on ventilation and thermal performance

Longitudinal pitch SL and transverse pitch ST (as shown in Fig. 15) are the dominant factors in terms of the ventilation and thermal performance. This section discusses the effect of the staggered arranged solid tubes with different SL and ST on fresh air rate, supply and indoor temperature.

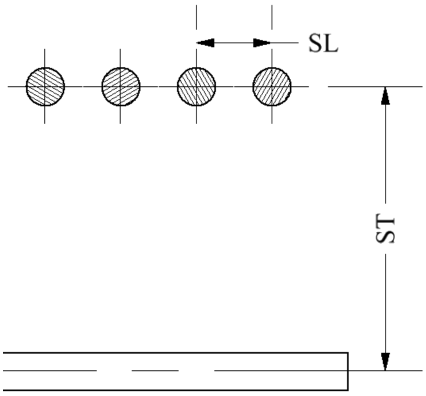

Fig. 15. The schematic of longitudinal pitch SL and transverse pitch ST

Effect of longitudinal pitch SL

As shown in Fig. 16, the temperature difference between the supply and the outdoor and fresh air rate is given with different SL varying from 25 mm to 45 mm. It can be seen that the supply temperature is incrased by reducing SL, so that the maximum supply temperature reaches up to 10.9 ℃ at the smallest SL=25 mm. Conversely, the fresh air rate shows an opposite trend with a minimum of 4.35 L/s/per person at the smallest SL=25 mm. Based on the results, it is suggested to reduce the SL as long as the system can provide sufficient fresh air rate.

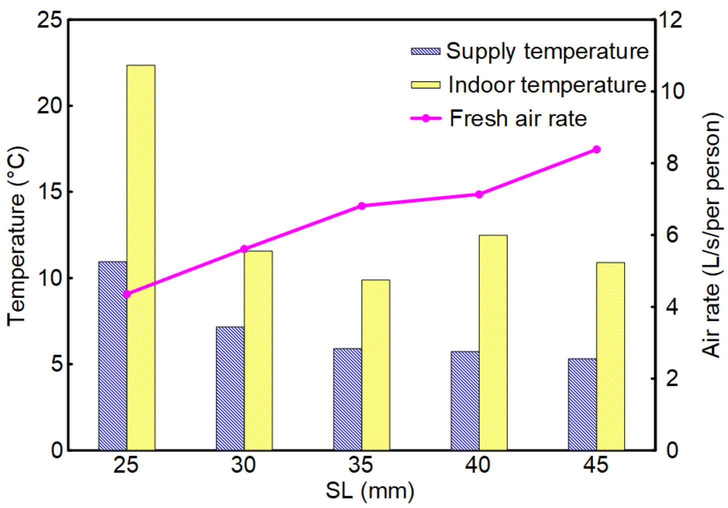

Fig. 16. Effect of varying SL on supply air temperature and fresh air rate

Effect of transverse pitch ST

As shown in Fig. 17, the supply temperature and fresh air rate are predicted for the proposed passive heat recovery wind tower with different ST, ranging from 60 mm to 180 mm. The results show a gradual decrease in supply temperature from 6.4 °C to 5.6 °C and a slight increase in fresh air rate from 3.71 L/s/per person to 3.94 L/s/per person as ST increases from 60 mm to 180 mm. Despite no noticeable difference in supply temperature and fresh air rate, a smaller ST that achieves maximum heat recovery with a reasonable pressure drop is recommended.

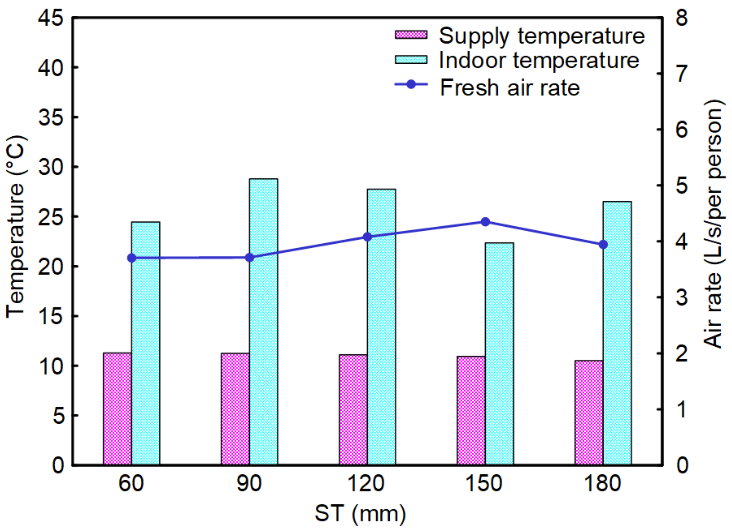

Fig. 17. Effect of varying ST on supply air temperature and fresh air rate

4.4 Effect of outdoor wind speed

Moreover, another study is carried out considering the effect of changing outdoor wind speed on the airflow velocity and system heat recovery performance. Assuming the wind direction angle 0°, Fig. 18 compares supply air temperature and fresh air rate of the wind tower with HR and the standard wind tower. It can be seen the outdoor wind speed is of great significance to the supply fresh air rate. The fresh air rate falls after incorporating the HR device into the wind tower . The fresh air rates are reduced by up to 52 L/s/per person at 5 m/s outdoor wind speed and 9 L/s/per person at 1m/s.

In addition, the higher the outdoor wind speed, the lower the supply air temperature. Based on the simulated conditions (5 ℃, 30 W/m^2), the supply air temperature in the wind tower with HR ranges from 5.21 ℃-11.3 ℃; while in the standard wind tower, the maximum supply air temperature is 5.17 ℃. The heat transfer recovery achieved by the addition of solid tube banks increases the air temperature as well as reduces ventilation heat loss. Based on the results, the ability of pre-heating supply fresh air for the wind tower with solid tube banks HR is comparable with that for the wind tower with passive heat recovery wheel with raising the supply air temperature by up to 2.8 ℃ [30], and is also competitive with the wind tower incorporated heat pipe heat recovery which is capable of raising the supply temperature by 4.5 K [28]. According to the building regulations, the occupant's minimum air supply rate is 10 L/s/person for a 15 people classroom. For the external wind speed of 1 m/s and below, the wind tower does not comply with this recommendation; however, when the external speed increases (3 m/s and above), the system exceeds the recommended value.

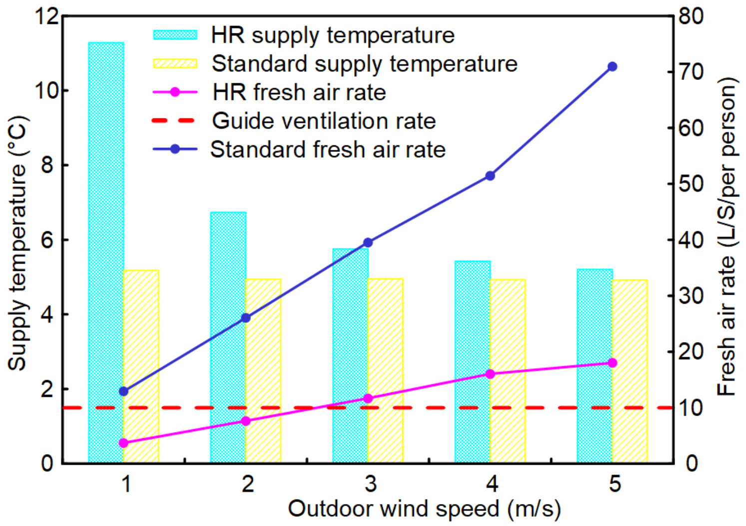

Fig. 18. Effect of varying external wind speeds on supply air temperature and fresh air rates

Fig. 19 displays effect of varying the outdoor wind speed (1-5 m/s) on the indoor air velocity and temperature for wind tower with HR and the standard wind tower. It was observed that after introducing the solid tube heat recovery device into the wind tower, the average indoor air temperature increased while the average indoor velocity is decreased. This could be a combined effect of reduced ventilation heat loss and heat transfer between the heat recovery device and airflow. With the increase of outdoor wind speed, , the indoor air temperature reduced, as shown in Fig 19b. It can be explained by the increased supply of fresh and cooler air causing enormous heat loss when the outdoor air is at a low temperature and high velocity. It is suggested to control the dampers at the bottom of the wind tower to reduce the fresh air volume if the outdoor wind speed is high. Compared with the heat pipes assisted wind tower in Ref. [28] achieving 5.3 ℃ increased in indoor air temperature, the proposed wind tower with solid tube bank heat recovery device also showed its potential for heat recovery with a temperature increased of up to 7.9 ℃.

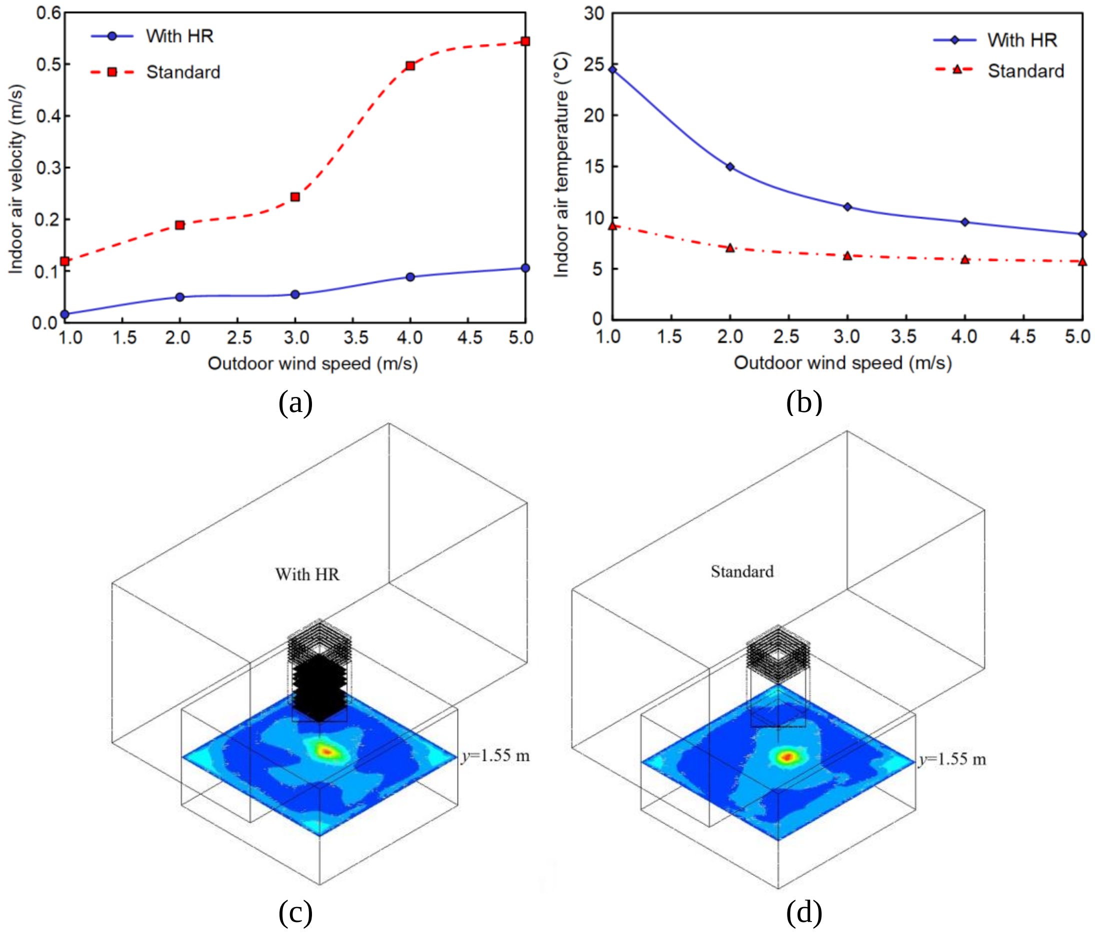

Fig. 19. Effect of varying external wind speeds on (a) indoor air velocity and (b) indoor air temperature; the characteristic plane (y=1.55 m) in (c) the standard tower and (d) the wind tower with HR

In order to examine the application of heat recovery device in detail, the estimated ventilation heating energy used for the building with a wind tower with no heat recovery and with heat recovery for a 5-h period at different outdoor wind speeds is predicted in Fig. 20. The building model's width, length, and height are 5 m, 5 m and 3 m respectively. The U values of roof, wall and floor are assumed as 0.18 W/m^{2}K, 0.26 W/m^{2}K, and 0.22 W/m^{2}K [30]. The indoor temperature is expected maintained at 21 ℃.

The building heating loss (Watts) is calculated as Eq. (1):

$$Q = (\sum (A \times U) + 0.33 \times N \times V) \times (T_\mathrm{i} - T_\mathrm{o}) \qquad (1)$$

where A is the building component area (m^2), U is the U value (W/m^{2}K), N is the air change rate (1/hour), V is the volume of building (m^3), T_i is the indoor temperature (K) and T_o is the outdoor temperature (K).

Substituting Eq. (1) into Eq. (2) can yield the required supply air temperature T_se.

$$Q = m \times c_\mathrm{p} \times (T_\mathrm{i} - T_\mathrm{se}) \qquad (2)$$

where c_p is the specific heat capacity of air (kJ/kg K) and m is the mass flow rate of air (kg/h).

The estimated ventilation heating energy W used over a period of t=5 h is calculated by Eq. (3):

$$W = t \times m \times c_\mathrm{p} \times (T_\mathrm{se} - T_\mathrm{sr}) \qquad (3)$$

where T_sr is the supply air temperature (K) after the HR device in the wind tower.

We assume that the outdoor temperature is kept at 5 ℃. During the 5 h period, when the outdoor speed increases from 1 m/s to 5 m/s, the heating energy demand of the building with the standard wind tower increases from 17.3 kWh to 103.9 kWh.

However, after adding the heat recovery devices, the heating energy demand is reduced, ranging from 0.2 kWh to 24.6 kWh. The heating requirement is significantly reduced due to the addition of heat recovery devices and the reduction of airflow velocity inside the wind tower.

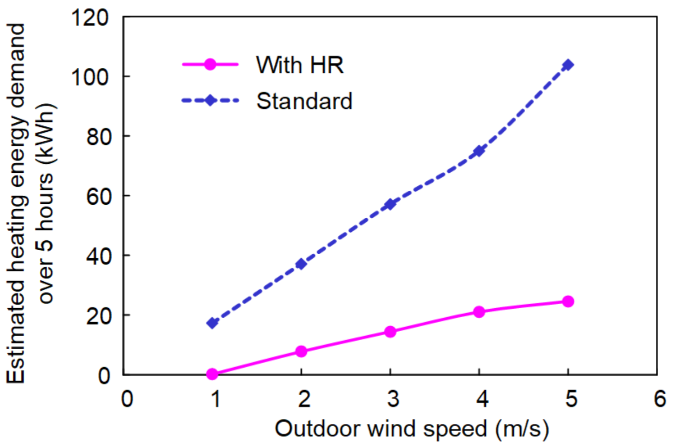

Fig. 20. Estimated ventilation heating energy: standard wind tower vs with HR (5 °C outdoor temperature)

5. Conclusions and future works

In this study, a four-sided wind tower system integrated with solid tube bank heat recovery device is proposed. The main challenge involves transferring energy from exhaust air to inlet airflow while meeting the guide ventilation rate for an occupied space. The overall aim is to improve the ability of wind tower to function throughout the year, especially in temperate climates with cool to cold winters. A three-dimensional CFD model is developed to simulate the airflow characteristics and heat recovery performance inside the wind tower with staggered solid pipes. The results demonstrate installing solid pipes can improve the heat transfer effect and can make wind tower function while reducing heat loss in the UK winter. As SL and ST are reduced to 25 mm and 60 mm respectively, the supply temperature reaches the maximum value of 11.28 °C. It is recommended to adopt smaller SL and ST if the required ventilation rate is met. This study also compared the influence of varying outdoor wind speed on the airflow and temperature distribution. When the external wind speed is from 1 m/s to 5 m/s, the supply temperature is reduced from 11.28 ℃ to 5.21 ℃ while the average supply velocity is increased from 0.22 m/s to 1.08 m/s. The CFD results show that the concept is feasible, but an experiment should be further conducted to validate the CFD predictions.

Acknowledgments: The support by the China Scholarship Council and University of Nottingham is gratefully acknowledged.

Nomenclature

Abbreviation

WHO	World Health Organization
CFD	Computational Fluid Dynamics
HR	Heat recovery
HVAC	Heating, Ventilation and Air-conditioning
EAHE	Earth-to-Air Heat Exchanger
CO_2	Carbon dioxide
RANS	Reynolds-averaged Navier-Stokes
LES	Large eddy simulation

Symbols

SL	Longitudinal pitch [mm]
ST	Transverse pitch [mm]
y+	Mesh specification near the wall (dimensionless)
V	Inlet velocity [m/s]
p	Static pressure [Pa]
T	Temperature [K, ℃]
g	Gravitational acceleration [m/s^2]
Q	Building heating loss [Watts]
A	Building component area [m^2]
U	U value [W/m^2K]
N	Air change rate [1/hour]
V	Volume of building [m^3]
m	Mass flow rate of air [kg/h]
c_p	Specific heat capacity of air [kJ/kg K]
W	Estimated ventilation heating energy [kWh]
D	Diameter of the tube

Subscript

i	Inlet
o	Outlet
se	Required supply air temperature
sr	Supply air temperature after the HR device

References

1 Ibn-Mohammed, T., Greenough, R., Taylor, S., Ozawa-Meida, L. and Acquaye, A., 2014. Integrating economic considerations with operational and embodied emis-

sions into a decision support system for the optimal ranking of building retrofit options. Building and Environment, 72, pp.82-101.
2 Deuble, M.P. and de Dear, R.J., 2012. Green occupants for green buildings: the missing link?. Building and Environment, 56, pp.21-27.
3 International Energy Agency, Birol F. World energy outlook 2013. Paris: International Energy Agency 2013.
4 van Ruijven, B.J., De Cian, E. and Wing, I.S., 2019. Amplification of future energy demand growth due to climate change. Nature Communications, 10(1), pp.1-12.
5 World Health Organization, 2020. World Health Organization Coronavirus Disease (COVID-19) Pandemic.
6 Fadaei, A., 2021. Ventilation Systems and COVID-19 Spread: Evidence from a Systematic Review Study. European Journal of Sustainable Development Research, 5(2), p.em0157.
7 Vassella, C.C., Koch, J., Henzi, A., Jordan, A., Waeber, R., Iannaccone, R. and Charrière, R., 2021. From spontaneous to strategic natural window ventilation: Improving indoor air quality in Swiss schools. International Journal of Hygiene and Environmental Health, 234, p.113746.
8 Kyritsi, E. and Michael, A., 2020. An assessment of the impact of natural ventilation strategies and window opening patterns in office buildings in the mediterranean basin. Building and Environment, 175, p.106384.
9 Wu, Y., Gao, N., Niu, J., Zang, J. and Cao, Q., 2021. Numerical study on natural ventilation of the wind tower: Effects of combining with different window configurations in a low-rise house. Building and Environment, 188, p.107450.
10 Sadeghi, M., Samali, B., Wood, G. and de Dear, R., 2020. Comfort cooling by wind towers in the Australian residential context–Experimental wind tunnel study of comfort. Journal of Wind Engineering and Industrial Aerodynamics, 196, p.104014.
11 Fini, A.S. and Moosavi, A., 2016. Effects of “wall angularity of atrium” on “buildings natural ventilation and thermal performance” and CFD model. Energy and Buildings, 121, pp.265-283.
12 Albuquerque, D.P., Mateus, N., Avantaggiato, M. and da Graça, G.C., 2020. Full-scale measurement and validated simulation of cooling load reduction due to nighttime natural ventilation of a large atrium. Energy and Buildings, 224, p.110233.
13 Taleb, H.M., Wriekat, T. and Hashaykeh, H., 2020. Optimising natural ventilation using courtyard strategies: CFD simulation of a G+ 1 office building in Madinah. International Journal of Sustainable Energy, 39(7), pp.659-684.
14 Al-Hemiddi, N.A. and Al-Saud, K.A.M., 2001. The effect of a ventilated interior courtyard on the thermal performance of a house in a hot–arid region. Renewable Energy, 24(3-4), pp.581-595.
15 Chatterjee, A., Zhang, L. and Xia, X., 2015. Optimization of mine ventilation fan speeds according to ventilation on demand and time of use tariff. Applied Energy, 146, pp.65-73.
16 Mouchtouri, V.A., Koureas, M., Kyritsi, M., Vontas, A., Kourentis, L., Sapounas, S., Rigakos, G., Petinaki, E., Tsiodras, S. and Hadjichristodoulou, C., 2020. Environmental contamination of SARS-CoV-2 on surfaces, air-conditioner and ventilation systems. International journal of hygiene and environmental health, 230, p.113599.

17 Zhai, Z.J., Johnson, M.H. and Krarti, M., 2011. Assessment of natural and hybrid ventilation models in whole-building energy simulations. Energy and Buildings, 43(9), pp.2251-2261.

18 Gao, R., Li, A., Hao, X., Lei, W., Zhao, Y. and Deng, B., 2012. Fire-induced smoke control via hybrid ventilation in a huge transit terminal subway station. Energy and Buildings, 45, pp.280-289.

19 Bahadori, M.N., 1985. An improved design of wind towers for natural ventilation and passive cooling. Solar Energy, 35(2), pp.119-129.

20 Bouchahm, Y., Bourbia, F. and Belhamri, A., 2011. Performance analysis and improvement of the use of wind tower in hot dry climate. Renewable Energy, 36(3), pp.898-906.

21 Farouk, M., 2020. Comparative study of hexagon & square windcatchers using CFD simulations. Journal of Building Engineering, 31, p.101366.

22 Chel, A. and Kaushik, G., 2018. Renewable energy technologies for sustainable development of energy efficient building. Alexandria Engineering Journal, 57(2), pp.655-669.

23 Sakhri, N., Moussaoui, A., Menni, Y., Sadeghzadeh, M. and Ahmadi, M.H., 2021. New passive thermal comfort system using three renewable energies: Wind catcher, solar chimney and earth to air heat exchanger integrated to real-scale test room in arid region (Experimental study). International Journal of Energy Research, 45(2), pp.2177-2194.

24 Moosavi, L., Zandi, M., Bidi, M., Behroozizade, E. and Kazemi, I., 2020. New design for solar chimney with integrated windcatcher for space cooling and ventilation. Building and Environment, 181, p.106785.

25 Benkari, N., Fazil, I. and Husain, A., 2017. Design and performance comparison of two patterns of wind-catcher for a semi-enclosed courtyard. International Journal of Mechanical Engineering and Robotics Research, 6(5), pp.396-400.

26 Benhammou, M., Draoui, B., Zerrouki, M. and Marif, Y., 2015. Performance analysis of an earth-to-air heat exchanger assisted by a wind tower for passive cooling of buildings in arid and hot climate. Energy Conversion and Management, 91, pp.1-11.

27 Ghoulem, M., El Moueddeb, K., Nehdi, E., Zhong, F. and Calautit, J., 2020. Analysis of passive downdraught evaporative cooling windcatcher for greenhouses in hot climatic conditions: Parametric study and impact of neighbouring structures. Biosystems Engineering, 197, pp.105-121.

28 Calautit, J.K., O'Connor, D. and Hughes, B.R., 2016. A natural ventilation wind tower with heat pipe heat recovery for cold climates. Renewable Energy, 87, pp.1088-1104.

29 Hughes, B.R., Chaudhry, H.N. and Calautit, J.K., 2014. Passive energy recovery from natural ventilation air streams. Applied Energy, 113, pp.127-140.

30 Calautit, J.K., O'Connor, D., Tien, P.W., Wei, S., Pantua, C.A.J. and Hughes, B., 2020. Development of a natural ventilation windcatcher with passive heat recovery wheel for mild-cold climates: CFD and experimental analysis. Renewable Energy, 160, pp.465-482.

31 Sangdeh, P. K., & Nasrollahi, N. (2020). Windcatchers and their applications in contemporary architecture. Energy and Built Environment.

32 Met Office, Weather Summaries 2015, 2014. Available on, http://www.metoffice.gov.uk/climate/uk/summaries/2014/annual.
33 Calautit, J.K. and Hughes, B.R., 2014. Wind tunnel and CFD study of the natural ventilation performance of a commercial multi-directional wind tower. Building and Environment, 80, pp.71-83.
34 Liu, Y., Yang, L., Hou, L., Li, S., Yang, J. and Wang, Q., 2017. A porous building approach for modelling flow and heat transfer around and inside an isolated building on night ventilation and thermal mass. Energy, 141, pp.1914-1927.
35 Nakhchi, M.E. and Esfahani, J.A., 2021. Numerical investigation of turbulent CuO–water nanofluid inside heat exchanger enhanced with double V-cut twisted tapes. Journal of Thermal Analysis and Calorimetry, 145(5), pp.2535-2545.
36 Sayed Ahmed, S.A.E., Mesalhy, O.M. and Abdelatief, M.A., 2015. Effect of longitudinal-external-fins on fluid flow characteristics for wing-shaped tubes bundle in crossflow. Journal of Thermodynamics, 2015.
37 Elmekawy, A.M.N., Ibrahim, A.A., Shahin, A.M., Al-Ali, S. and Hassan, G.E., 2021. Performance enhancement for tube bank staggered configuration heat exchanger–CFD Study. Chemical Engineering and Processing-Process Intensification, 164, p.108392.
38 Blocken, B., 2018, October. LES over RANS in building simulation for outdoor and indoor applications: a foregone conclusion?. In Building Simulation (Vol. 11, No. 5, pp. 821-870). Springer Berlin Heidelberg.
39 Jiang, Y. and Chen, Q., 2002. Effect of fluctuating wind direction on cross natural ventilation in buildings from large eddy simulation. Building and environment, 37(4), pp.379-386.
40 Blocken, B., Stathopoulos, T. and Van Beeck, J.P.A.J., 2016. Pedestrian-level wind conditions around buildings: Review of wind-tunnel and CFD techniques and their accuracy for wind comfort assessment. Building and Environment, 100, pp.50-81.
41 Blocken, B., 2015. Computational Fluid Dynamics for urban physics: Importance, scales, possibilities, limitations and ten tips and tricks towards accurate and reliable simulations. Building and Environment, 91, pp.219-245.
42 van Hooff, T., Blocken, B. and Tominaga, Y., 2017. On the accuracy of CFD simulations of cross-ventilation flows for a generic isolated building: comparison of RANS, LES and experiments. Building and Environment, 114, pp.148-165.
43 Peren, J.I., Van Hooff, T., Ramponi, R., Blocken, B. and Leite, B.C.C., 2015. Impact of roof geometry of an isolated leeward sawtooth roof building on cross-ventilation: Straight, concave, hybrid or convex?. Journal of Wind Engineering and Industrial Aerodynamics, 145, pp.102-114.
44 Ramponi, R. and Blocken, B., 2012. CFD simulation of cross-ventilation for a generic isolated building: impact of computational parameters. Building and environment, 53, pp.34-48.
45 Ahmadi, M., 2020. How the Position of a Root-Top One-Sided Wind Tower Affects Its Cross-Ventilation Effectiveness. In Sustainability in Energy and Buildings (pp. 469-479). Springer, Singapore.
46 Tominaga, Y., Akabayashi, S.I., Kitahara, T. and Arinami, Y., 2015. Air flow around isolated gable-roof buildings with different roof pitches: Wind tunnel experiments and CFD simulations. Building and Environment, 84, pp.204-213.
47 Ferziger, J.H., 1990. Approaches to turbulent flow computation: applications to flow over obstacles. Journal of Wind Engineering and Industrial Aerodynamics, 35, pp.1-19.